Impact of flow unsteadiness on steady-state gas-path stagnation temperature measurements

Clare Bonham, Mark Brend, Adrian Spencer, Katsu Tanimizu and Dylan Wise*
Department of Aeronatutical and Aeronautical Engineering
Loughborough University
Loughborough, UK
Email: c.bonham@lboro.ac.uk

Steady-state stagnation temperature probes are used during gas turbine engine testing as a means of characterising turbomachinery component performance. The probes are located in the high-velocity gas-path, where temperature recovery and heat transfer effects cause a shortfall between the measured temperature and the flow stagnation temperature. To improve accuracy, the measurement shortfall is corrected post-test using data acquired at representative Mach numbers in a steady aerodynamic calibration facility. However, probes installed in engines are typically subject to unsteady flows, which are characterised by periodic variations in Mach number and temperature caused by the wakes shed from upstream blades. The present work examines the impact of this periodic unsteadiness on stagnation temperature measurements by translating probes between jets with dissimilar Mach numbers. For conventional Kiel probes in unsteady flows, a greater temperature measurement shortfall is recorded compared to equivalent steady flows, which is related to greater conductive heat loss from the temperature sensor. This result is important for the application of post-test corrections, since an incorrect value will be applied using steady calibration data. A new probe design with low susceptibility to conductive heat losses is therefore developed, which is shown to deliver the same performance in both steady and unsteady flows. Measurements from this device can successfully be corrected using steady aerodynamic calibration data, resulting in improved stagnation temperature accuracy compared to conventional probe designs. This is essential for resolving in-engine component performance to better than $\pm 0.5\%$ across all component pressure ratios.

Nomenclature

A area
C specific heat capacity
D probe duty cycle
f frequency
h heat transfer coefficient
k thermal conductivity
m mass
M Mach number
Nu Nusselt number
P static pressure
$P0$ stagnation pressure
Pr Prandtl number
R characteristic gas constant
Re Reynolds number
R_T temperature recovery ratio
t time
T static temperature
$T0$ stagnation temperature
U velocity
V volume

Greek symbols

$\varnothing$ diameter
γ specific heat ratio
λ temperature recovery factor (adiabatic)
μ viscosity
η efficiency
ρ density
τ sensor time constant

Subscripts

aw adiabatic wall
b thermocouple bead
g gas
i inner jet
in inlet
max maximum
o outer jet
out outlet
p polytopic
∞ free-stream

*Present address: Department of Engineering Science, University of Oxford, Southwell Building, Osney Mead, Oxford OX2 0ES, UK

1 INTRODUCTION

The accurate measurement of steady-state gas-path stagnation temperatures is an important aspect of gas turbine engine testing. The measurements are used to characterise the engine running condition and to assess the performance of individual components of turbomachinery. High accuracy is important since small uncertainties in stagnation temperature result in large changes in calculated component efficiency. Eqn. 1 shows how the isentropic efficiency of a compressor can be determined from gas-path stagnation temperature measurements, together with knowledge of the component pressure ratio:

$$\eta = \frac{\left[\frac{P0_{out}}{P0_{in}}\right]^{\frac{\gamma-1}{\gamma}} - 1}{\left[\frac{T0_{out}}{T0_{in}}\right] - 1} \tag{1}$$

To continue the development of more efficient engines with reduced specific fuel consumption, aero engine manufacturers are currently seeking improvements in component efficiency of $< 1\%$. This has led to a desire to reduce the uncertainty associated with efficiency assessments to $\pm 0.5\%$. In order to achieve this level of accuracy, an analysis of Eqn. 1 shows that absolute stagnation temperature uncertainties of $\leq \pm 0.1\%$ are required [1]. This includes contributions from probe temperature recovery ratio corrections as well as the sensor and data acquisition system performance. Sufficiently high accuracy is most difficult to achieve in low pressure ratio components such as the fan of a high-bypass ratio turbofan, since any uncertainty represents a larger proportion of the overall stagnation temperature rise [2]. In the fan, near-ambient gas-path temperatures place the target measurement uncertainty at $< \pm 0.3\,K$.

Stagnation temperature measurements are typically acquired using Kiel probes, which are comprised of thermocouple sensors housed within passively-ventilated stagnation tubes (see Fig. 1). The thermocouples can either be open bead or mineral insulated, with junction diameters of $< 1\,mm$. The stagnation tube is provided around the thermocouple to reduce sensitivity to temperature recovery effects by decelerating the flow over the sensor to a low velocity. However, this arrangement reduces the convective heat transfer to the thermocouple and causes the probe to become sensitive to conductive and radiative heat transfer to the surroundings [3]. At steady-state, the probe measured temperature is therefore determined by the balance of heat fluxes at the thermocouple junction. The heat balance is a function of flow Mach number, since this changes the convective heat transfer coefficient to the thermocouple junction as well as the temperature gradient driving conduction. The difference between the probe measured temperature and the true flow stagnation temperature is characterised by the temperature recovery ratio:

$$R_T = \frac{T_b}{\widetilde{T0}_\infty} \tag{2}$$

To improve stagnation temperature accuracy, Saravanamuttoo [2] recommends correcting probe indicated temperatures using recovery ratios obtained from aerodynamic calibrations. These calibrations are typically performed in an atmospheric free-jet at gas-path representative Mach numbers. However, there are differences between the engine and calibration environments that can lead to uncertainties in the post-test corrections applied. One important difference is the flow unsteadiness that is introduced by rotating turbomachinery. This unsteadiness is characterised by fluctuations in pressure, temperature, velocity and flow angle that have stochastic as well as periodic components [4]. The stochastic fluctuations arise due to turbulent effects, while the periodic fluctuations are predominately associated with wakes shed from passing blades. This places the frequency content of the unsteadiness at between 3 and 30 kHz [5].

Kiel probes have insufficient dynamic response to resolve such high frequency fluctuations, therefore the probe measured temperature assumes a quasi-steady state [6]. This is primarily a consequence of the frequency sensitivity of commercially available thermocouples, which is limited to values of the order 10 Hz due to the size of the junction diameter [7]. The presence of the stagnation tube reduces this frequency sensitivity further as a result of its large thermal inertia and low thermal diffusivity [8]. Instruments are available that can respond dynamically at higher frequencies than Kiel probes, but many use fine wire sensing elements [9] that are not sufficiently robust for use in an engine test environment. More robust devices based on thin-film [10] and fibre optic [11] sensors also exist, but are typically associated with unacceptably large measurement uncertainties for engine performance measurements. The same is true for optical techniques such as tunable diode laser absorption spectroscopy (TDLAS), which also necessitates the provision of special viewing windows or fibre-optics [12].

For Kiel probes located in compressor wake flows, the relationship between the quasi-steady probe measured temperature and the average flow stagnation temperature has been studied by Moffat [6], Agnew et al. [13] and Bianchini et al. [14]. These studies suggest that the probe struggles to indicate the average flow temperature due to biasing influences that cause temperatures inside and outside of the wake to be weighted by different amounts. According to Moffat [6], the convective heat transfer coefficient represents an important biasing influence, since it varies non-linearly with the fluctuating flow velocity across the wake. Selective sampling processes imposed by the design of the stagnation tube may also be a significant factor [13]. Under unsteady flow conditions, the difference between the probe measured temperature and the average stagnation temperature will therefore be altered compared to equivalent steady flow conditions. This raises concerns over the accuracy of post-test correc-

tions based on steady aerodynamic calibration data, which necessarily exclude unsteady effects.

To achieve the best stagnation temperature accuracy, the impact of unsteady effects on probe measured temperatures must be reduced. Agnew et al. report that this can be achieved by locating the probe far downstream of rotating blades, where the flow unsteadiness has mixed out [13]. However, it is current convention to mount Kiel probes to the stator leading edge, which limits the amount of axial adjustment that is practically achievable. If sufficient information is known about the probe and flow field, attempts could alternatively be made to correct for unsteady effects using analytical models. This has previously been attempted by Bianchini et al. [14], but has enjoyed limited success due to the propagation of uncertainties in the unsteady flow conditions to the measurement correction. In addition, the time-resolved flow field measurements required for such corrections are not routinely acquired during gas turbine engine testing due to constraints on instrumentation space. A final approach is therefore to identify probe designs that are insensitive to unsteadiness, such that the difference between the measured temperature and average flow stagnation temperature remains constant under equivalent steady and unsteady conditions. This is the aim of the current work.

2 EXPERIMENTAL TEST FACILITY

Figure 2 shows normalised flow profiles downstream of the fan of a high bypass ratio turbofan engine, at a location where Kiel probes are typically installed during engine performance testing. This data has been obtained from unsteady CFD simulations performed by Rolls-Royce plc. The flow structure can be described by a jet and wake, where the minimum Mach number in the wake is 80% of the Mach number in the jet. The absolute stagnation temperature remains constant to within $\leq 0.5\%$ between the jet and wake. Based on the isentropic temperature equation, the absolute static temperature in the wake therefore rises by around 4% due to the Mach number deficit. These periodic fluctuations in Mach number and temperature occur at the blade passing frequency, which is of the order 1 kHz. The fluctuations are nominally in-phase with each other and extend over 30% of the circumferential blade pitch.

Experiments to investigate stagnation temperature probe performance under conditions characteristic of those in Fig. 2 are complicated by the requirement to accurately measure the reference properties of the flow. This necessitates the application of fast-response measurement techniques, such as those described in [9], [10] and [11]. Both Agnew et al. [13] and Bianchini et al. [14] have reported difficulties in this undertaking, which raises questions over the reliability of the results obtained. As a consequence, the present investigation uses an alternative approach whereby the probe under test is translated between multiple steady flows. This allows the reference flow properties to be measured using conventional steady-state techniques, which are associated with higher accuracy.

Figure 3 shows a schematic diagram of the current test facility. It is supplied with air by two Kaeser screw compressors that can pressurise up to 1 kg/s of ambient air to 14 bar. Two parallel 6" diameter pipelines deliver the compressed air to coaxial, coplanar nozzles that exhaust to atmosphere. The nozzle design was originally developed as part of the CoJeN (Coaxial Jet Noise) project with guidance from Rolls-Royce [15]. It is used here at approximately 1/25th of engine scale, with an inner (primary) nozzle diameter of 40 mm and an outer (secondary) nozzle diameter of 80 mm. The stagnation temperature is fixed by ambient conditions and remains constant between the two jets. The Mach number of the jets can be independently controlled using a pair of Spirax Sarco globe valves, which are located in the 6" diameter flow delivery pipelines. Figure 4 shows the velocity profile across the nozzles for three different combinations of inner and outer jet Mach number. These measurements have been determined from a stereoscopic particle image velocity (PIV) survey of the jet flows. 2000 statistically independent samples were measured using a bespoke PIV system, developed in house. The data presented was processed using the LaVision DaVis V8.2 to recover average velocity fields from these samples.

The probe under test is positioned 40 mm downstream of the nozzle throat and connected to a crank-driven linear slide. The slide is used to translate the probe between the two coaxial jets in order to impose fluctuations in Mach number and static temperature that are characteristic of the wake conditions pictured in Fig. 2. Table 1 summarises the test conditions that can be achieved with different combinations of inner and outer jet Mach number. Over one complete revolution of the crank shaft, the displacement of the probe follows a near-sinusoidal profile with 20 mm amplitude (peak-peak). By aligning the 0 mm probe position with the boundary between the two jets ($\pm 20\,mm$ from the nozzle centreline), a nominal $50/50$ duty cycle can be achieved where the probe crosses each jet for half of traverse cycle. Other duty cycles can be attained by shifting the 0 mm probe position into the potential core of one of the jets. The rotational speed of the crankshaft can be adjusted to set the probe translation frequency, which is limited to $\leq 40\,Hz$. This is two orders of magnitude below typical fan blade passing frequencies ($1\,kHz$) and represents the principal drawback of the current experiential approach.

The reference stagnation pressure and temperature in each jet is measured in the flow delivery pipework upstream of the nozzles. In this region, flow velocities are sufficiently low ($\leq$ Mach 0.15) that pressure and temperature recovery effects are small. Stagnation temperatures are measured using commercially available passively aspirated thin-film PRT probes, which are connected in 4-wire mode to a Pico PT-104 resistance measuring instrument. Stagnation pressures are measured using Pitot tubes, which are connected to a pair of Huba controls 691 series absolute pressure transducers. A third absolute pressure transducer is used to measure the static pressure in the laboratory, which is required to calculate jet Mach numbers from the isentropic pressure relation. Temperature measurements from the probe under test are acquired using either a National Instruments SCXI-1120 (ex-

ternal 0^oC cold junction) or a Pico PT-104 for thermocouple and PRT based devices respectively.

Prior to use in the test facility, all instrumentation is statically calibrated against an appropriate traceable standard. The systematic measurement uncertainties are estimated from the residual uncertainty in the calibration standard, plus the installed uncertainty associated with the measuring environment. Random measurement uncertainties are determined by calculating the standard deviation of repeated static calibrations and then applying the Student's t-distribution. Using the Taylor series method of uncertainty propagation, the measurement uncertainties can be used to determine uncertainties in derived variables, including temperature recovery ratio (Eqn. 2) and Mach number (Eqn. 11) [16]. These values are summarised in Tab. 2 for a 50/50 duty cycle with an inner jet Mach number of 0.6 and an outer jet Mach number of 0.3. The Mach number sensitivity in the reference measurements arises from small pressure and temperature recovery effects, which are related to the installation of the probes in the upstream pipework.

3 FREQUENCY EFFECTS

To understand the importance of the frequency limitations in the proposed experimental approach, a first order analysis of the probe's dynamic response has been performed. Olczyk [17] has previously used a lumped capacitance approach to model the dynamic response of an open bead thermocouple in an unsteady flow. The approach treats the bead as a homogeneous isolated sphere and assumes that temperature gradients within the bead are negligible at any instant in time. This condition is satisfied by the small diameter ($\leq 1\,mm$) and high thermal conductivity ($\sim 20\,W/mK$ for N-type devices) of the bead. The rate of change of the bead's internal energy is equated to the rate of convective heat transfer from the adjacent fluid, neglecting the effects of conductive and radiative heat transfer to the surroundings.

$$m_b C_b \frac{dT_b}{dt} = hA_b(T_{aw} - T_b) \tag{3}$$

Eqn. 3 describes a first order system and can be expressed in the more familiar form:

$$T_{aw} = T_b + \tau \frac{dT_b}{dt} \tag{4}$$

where τ is the thermocouple time constant:

$$\tau = \frac{m_b C_b}{hA_b} \tag{5}$$

The parameter $m_b C_b$ is defined as the thermal capacity of the thermocouple and is calculated from the physical properties of the bead. A high thermal capacity is associated with a long time constant and a slow dynamic response. The convective heat flux to the thermocouple is proportional to the difference between the actual surface temperature of the bead and the adiabatic wall temperature. The convective heat transfer coefficient h can be expressed in the form of a Nusselt number, which is determined from Whitaker's correlation for flow over a sphere [18]:

$$Nu = 2 + (0.4Re^{0.5} + 0.06Re^{2/3})Pr^{0.4} \tag{6}$$

where

$$Nu = \frac{h\varnothing_b}{k_g},\ Re = \frac{\rho U \varnothing_b}{\mu},\ Pr = \frac{C_g \mu}{k_g} \tag{7}$$

The heat transfer coefficient is evaluated for conditions inside the Kiel probe, local to the thermocouple bead. The Mach number at this location can be related to the free-stream Mach number using Eqn. 8, which is a function of the flow areas at inlet and outlet of the Kiel shroud [2]. This assumes free-stream static conditions at the vent holes and stagnation conditions within the Kiel:

$$M = \frac{U}{\sqrt{\gamma RT}} = M_\infty \left(\frac{A_{out}}{A_{in}}\right) \left[1 + \frac{\gamma - 1}{2} {M_\infty}^2\right]^{\frac{-1}{\gamma - 1}} \tag{8}$$

Assuming stagnation pressure and temperature are conserved, the static properties inside the Kiel can be determined from this local Mach number using the isentropic flow equations. This allows the properties of the flow inside the Kiel (ρ, C_g, μ, k_g) to be calculated from ideal gas equations.

Figure 5 shows the response of a $0.5\,mm$ diameter N-type thermocouple bead to the fan blade wake conditions illustrated in Fig. 2. For this device, τ is estimated at $\sim 1\,s$ from Eqn. 5. For fan blade passing frequencies $<< \frac{1}{\tau}$, the thermocouple responds dynamically to the temperature fluctuation across the wake. Due to the thermal capacity of the sensor, the bead temperature lags the wake temperature and attains a consistently lower amplitude. For blade passing frequencies $>> \frac{1}{\tau}$, the thermocouple no longer responds dynamically to the fluctuating wake flow and the bead temperature converges towards a fixed value. This result has significant implications for the experimental approach outlined in section 2, since it implies that the frequency range of interest for an isolated thermocouple bead is limited to $0 - 10\,Hz$. For a Kiel probe, this range will be further reduced by the presence of the stagnation tube, which has large thermal inertia and low thermal diffusivity [8]. The maximum $40\,Hz$ translation frequency that is achievable with the crank-driven linear slide will therefore be sufficient for determining probe performance under unsteady flow conditions.

4 MECHANICAL EFFECTS

There are other advantages associated with limiting probe traverse frequencies to values $\leq 40Hz$. For example, forces acting on the probe will increase with frequency and may cause damage to occur. One potential issue surrounds straining of the sensing element, which could result in changes to its thermoelectric response at relatively low forcings. To investigate this possibility, candidate probes were mounted to an electro-dynamic shaker and vibrated at a frequency of $100Hz$ ($20g$). Initial static calibrations were performed and repeated after 3, 6, and 9 hours of vibration. The results of this process are plotted in Fig. 6, which shows the change in probe indicated temperature relative to the initial calibration at a nominal temperature of 20^oC. A maximum temperature change of 0.02^oC is recorded, which is within the uncertainty of the measurement system (see Tab. 2). Traverse frequencies in the experimental range of $\leq 40Hz$ are therefore unlikely impact on sensor static calibration retention.

The incidence angle between the probe and oncoming flow will also become greater as the probe translation frequency is increased. Figure 7 plots this incidence angle for a range of translation frequencies and jet Mach numbers, based on the maximum probe velocity during the traverse cycle. Angles of $\leq 3.5^o$ are calculated across all conditions, which suggests that probe performance is unlikely to be influenced by incidence effects. Kiel probes are designed for angular insensitivity and typically only experience changes in performance beyond $\pm 15^o$, where flow separation occurs [6].

5 TEST DATA REDUCTION

The performance of the stagnation temperature probe under test is quantified by the temperature recovery ratio. This is calculated from Eqn. 2 using measurements of the probe indicated temperature and the reference stagnation temperature. Given that the probe under test traverses between two jets, the reference stagnation temperature must be based on an average value. Since component efficiencies should be calculated using mass-flux weighted stagnation temperatures, this is the averaging approach that will be adopted [19]:

$$\widetilde{T0}_\infty = \frac{\rho_i U_i T0_i D + \rho_o U_o T0_o (1-D)}{\rho_i U_i D + \rho_o U_o (1-D)} \tag{9}$$

D is the probe duty cycle, which is defined as:

$$D = \frac{A_1}{A_1 + A_2} \tag{10}$$

A_1 and A_2 represent areas enclosed by a non-dimensionalised plot of jet velocity against time, which is derived from the PIV measurements in Fig. 4. Figure 8 is an example of such a plot for a probe operating on a nominal 50/50 duty cycle. Since PIV measurements are unavailable for the full range of test conditions listed in Tab. 1, the velocity profile is constructed using a three-part curve fit. Constant jet velocities are prescribed across the two potential cores, while a half-period sinusoid is used to represent the dividing shear layer. Changes in shear layer thickness with Mach number are accounted for by linearly interpolating the PIV measurements and adjusting the amplitude of the sinusoid accordingly. This approach enables the areas A_1 and A_2 to be evaluated by definite integration, with unique duty cycles obtained for each test condition.

Using a similar methodology, the duty cycle can also be used to calculate the average jet Mach number. This information is necessary for producing calibration curves of temperature recovery ratio against Mach number, which are used as the basis for applying post-test corrections to engine measurements. A simple time-average Mach number is used rather than a mass-flux weighted Mach number since this value is unlikely to be known in the engine gas-path.

$$\bar{M}_\infty = M_i D + M_o (1-D) \tag{11}$$

6 TEST RESULTS

For three different Kiel probe designs, comparisons have been made of stagnation temperature measurement performance under steady and unsteady flow conditions. Unsteady data has been obtained with the probe traversing between coaxial jets with different Mach numbers at a range of frequencies and duty cycles. Steady data has been acquired with the probe held stationary on the centre-line of the inner jet. The probes selected are all based on designs intended for use at measurement stations downstream of the fan of a high-bypass ratio turbofan engine.

6.1 Thermocouple Kiel

The first probe to be considered is a thermocouple Kiel, similar to that pictured in Fig. 1. The probe consists of a thermocouple sensor, which is housed within a passively ventilated stainless-steel stagnation tube. This design represents the current standard for stagnation temperature measurements in gas turbine engines. Figure 9 shows histograms of the temperature indicated by the thermocouple Kiel probe under unsteady test conditions. This data was obtained with a jet Mach number ratio (M_o/M_i) of 0.33 at probe traverse frequencies of 0.5 Hz and 10 Hz. At 0.5 Hz, the histogram contains two distinct temperature peaks that correspond to the different measurement conditions in the two coaxial jets. At 10 Hz, these differences are no longer detected and the histogram is comprised of a single temperature peak that represents an average of the conditions across the two jets. The differences in absolute temperature between the two plots relate to day-to-day variations in ambient conditions, which set the jet stagnation temperature. This result is in broad agreement with the first order model described in section 3, which

predicts that the dynamic response of the probe will be limited to frequencies $<< \frac{1}{\tau}$. For the thermocouple Kiel, τ is estimated at $\sim 1\,s$ using Eqn. 5. This confirms that unsteady testing can be sensibly restricted to frequencies in the range $1-10\,Hz$, as predicted in section 3.

Figure 10 compares temperature recovery ratios for the thermocouple Kiel probe determined under steady (0 Hz) and unsteady test conditions. The unsteady data corresponds to probe traverse frequencies up to 30 Hz and a nominal 50/50 duty cycle. For a given time-average Mach number, the probe temperature recovery ratio remains constant for traverse frequencies $\geq 1\,Hz$. However, there is a clear reduction in temperature recovery ratio between the steady and unsteady test cases. In unsteady conditions, this implies that there is a greater shortfall between the probe indicated temperature and the average flow stagnation temperature compared to that in steady conditions. This outcome has important implications for stagnation temperature accuracy, since there will be an error in the corrected temperature if recovery ratios based on steady aerodynamic calibrations are used to adjust measurements in unsteady flows. In turbomachinery applications, this error would lead to an incorrect calculation of component performance from Eqn. 1. Since this information is ultimately used to guide engine development efforts, this could mistakenly result in design refinements being targeted at the wrong components, with significant implications for project costs and time.

Figure 11 shows the change in probe indicated temperature between equivalent steady and unsteady test conditions (constant $\bar{M}_\infty$) for 50/50 and 70/30 duty cycles, at a probe traverse frequency of $10\,Hz$. The greatest changes are observed at the highest time-average Mach numbers, which correspond to large Mach number fluctuations between the inner and outer jets. At a given time-average Mach number, the temperature change is also greater for the 50/50 duty cycle compared to the 70/30 cycle. In turbomachinery flows, it is therefore expected that the impact of flow unsteadiness on probe indicated temperature will be greatest where there is a large Mach number deficit between the jet and wake, and where the wake extends across a large percentage of the circumferential blade pitch. This will depend on factors including the aerodynamic design of the blades (e.g. thickness to chord ratio), as well as the mixing that takes place upstream of the probe. Consequently, a particular probe design will perform differently depending on the precise characteristics of the wake flow at the measurement location. This makes any attempt to correct for unsteady effects extremely difficult.

Figure 12 shows the influence of stagnation temperature uncertainties on the isentropic efficiency of a compressor. These values have been calculated using Eqn. 1 for a range of pressure ratios and an inlet stagnation temperature of $300\,K$. To illustrate the potential impact of unsteady effects, an uncertainty of $0.26\,K$ ($0.09\%T0_\infty$) has been selected based on the changes in probe indicated temperature plotted Fig. 11. This value corresponds to a 70/30 duty cycle and a time-average Mach number of ~ 0.6, which are considered to be representative of a turbomachinery flow. The impact of this uncertainty on component efficiency decreases with pressure ratio, since it represents a successively smaller proportion of the overall temperature rise. However, for pressure ratios < 2 uncertainties in efficiency of $> 0.5\%$ are observed, which would make incremental improvements in component performance difficult to detect. This is of particular importance for the fan of a high-bypass ratio turbofan engine, where pressure ratios are in the range $1.4-1.8$. The uncertainty in calculated component efficiency becomes even greater if additional sources of stagnation temperature uncertainty are added to unsteady effects, such as the fundamental sensing accuracy of the thermocouple. At near-ambient conditions, this can contribute an additional $0.81\,K$ to the stagnation temperature uncertainty [1]. Combining these values using a root-sum-square method leads to an overall stagnation temperature uncertainty of $0.84\,K$ ($0.28\%T0_\infty$). This results in uncertainties in efficiency of $> 1.5\%$ for low pressure ratios typical of a fan, and $> 0.5\%$ for higher pressure ratios ($2.5-10$) characteristic of core compressors. In order to assess efficiencies to within the target accuracy of $\pm 0.5\%$, reductions in the stagnation temperature uncertainties introduced by both sensor performance and unsteady effects are therefore required.

6.2 PRT Kiel

The second probe to be considered in this study is a PRT Kiel, which is shown in Fig. 13. This device adopts the same stagnation tube design as the thermocouple Kiel, but features a thin-film PRT in place of the thermocouple sensor. Thin-film PRTs offer higher fundamental measurement accuracy compared to thermocouples as a consequence of their better static calibration retention, higher signal to noise ratio and provision of absolute (rather than differential) temperature measurements [20]. At near-ambient conditions, these characteristics result in a temperature measurement uncertainty of $0.15\,K$, compared to $0.81\,K$ for thermocouples [1]. By adopting a PRT sensor in place of a thermocouple, the dominant source of stagnation temperature uncertainty in Fig. 12 will therefore be reduced. This makes the probe particularly advantageous for use in low pressure ratio components, where the impact of stagnation temperature uncertainties is greatest. This application complements the PRT's temperature rating, which is limited to approximately $750\,K$.

Temperature recovery ratios for the PRT Kiel probe are plotted in Fig. 14 for steady and unsteady test conditions. Unsteady data is shown for a range of probe traverse frequencies and a nominal 50/50 duty cycle. In common with the thermocouple Kiel, probe temperature recovery ratios are reduced under unsteady test conditions but remain constant for traverse frequencies $\geq 1\,Hz$. Figure 15 shows the corresponding changes in probe indicated temperature between the steady and unsteady tests. Similar temperature changes are observed compared to those for the thermocouple Kiel in Fig. 11, hence a similar error will remain in corrected temperatures following the application of steady aerodynamic calibration data. For a 70/30 duty cycle and a time-average Mach number of ~ 0.6, this is $0.26\,K$ ($0.09\%T0_\infty$). However,

since the fundamental accuracy of PRT sensors is reduced to $0.15K$, the combined stagnation temperature uncertainty for the PRT Kiel decreases to $0.30K$ ($0.10\%T0_\infty$). This compares to $0.84K$ ($0.28\%T0_\infty$) for the thermocouple Kiel. In turbomachinery applications, more accurate assessments of component efficiency would consequently be possible, but from Eqn. 1 it can be shown that uncertainties greater than the target of $\pm 0.5\%$ would still persist at typical fan pressure ratios < 2. Since the stagnation temperature uncertainty is now dominated by unsteady effects, the probe's sensitivity to unsteadiness must be addressed if accuracy is to be further improved.

6.3 Acrylic PRT Kiel

When thermal radiation is insignificant ($< 900K$), the temperature indicated by a stagnation temperature probe is determined by the balance between conductive and convective heat fluxes at the sensing element [21]. In unsteady test conditions, both of these heat fluxes undergo changes due to the fluctuating jet Mach number. The convective heat transfer coefficient varies non-linearly with Mach number due to the relationship between Reynolds and Nusselt numbers, which typically takes the form:

$$Nu = f(Re^{\alpha} Pr^{\beta}) \tag{12}$$

where α and β are constants < 1

Based on this relationship, the average heat transfer coefficient to the sensor under unsteady conditions can be shown to reduce compared to that under equivalent steady conditions (since $\alpha, \beta < 1$). This reduction is greater when the velocity fluctuation is large and persists for a long duration. However, the magnitude of the reduction is always minor ($\sim 1\%$) since the associated changes in Reynolds number inside the stagnation tube are small [6]. The impact on the probe measured temperature and hence recovery ratio are therefore minimal.

The conductive heat flux also varies non-linearly with Mach number since it is driven by a temperature gradient between near-stagnated flow at the sensor ($\sim T0_\infty$) and high-velocity flow travelling over the external surface of the probe (T_{aw}). The recovery temperature acting on the probe surface is a function of the adiabatic temperature recovery factor of the probe body and the free-stream static temperature, which can be related to Mach number through Eqn. 13 and Eqn.14:

$$T_{aw} = \lambda(T0_\infty - T_\infty) + T_\infty \tag{13}$$

where

$$\frac{T0_\infty}{T_\infty} = 1 + \frac{1}{2}(\gamma - 1)M_\infty^2 \tag{14}$$

Using these equations, the average temperature gradient driving conduction can be shown to increase by $\sim 10\%$ under unsteady test conditions compared to equivalent steady conditions ($\bar{M}_\infty$, $\bar{T0}_\infty$). Greater conductive heat losses are therefore incurred in the unsteady case, which are thought to be the leading cause of the lower probe indicated temperatures and recovery ratios reported in sections 6.1 and 6.2. Again, this effect is greater when the velocity fluctuation is large and persists for a long duration. Based on this hypothesis, the impact of unsteadiness on probe performance should be reduced for designs with low sensitivity to thermal conduction. An example of such a probe design is the acrylic PRT Kiel, which employs a stagnation tube constructed from low thermal conductivity acrylic ($k = 0.2W/mK$) in order to reduce heat losses from the temperature sensor. This design is geometrically similar to the metallic PRT Kiel described in section 6.2 (to within manufacturing tolerances). Any differences in probe performance can consequently be attributed to a reduction in conductive heat loss between the two devices.

Figure 16 shows temperature recovery ratios determined for the acrylic PRT Kiel probe under both steady and unsteady test conditions. Results are included for $50/50$ and $70/30$ duty cycles at a single traverse frequency ($10Hz$), since no frequency sensitivity is observed beyond $1Hz$. Compared to the standard PRT Kiel, the differences in temperature recovery ratio between steady and unsteady test conditions are small. From Fig. 17, these differences can be seen to correspond to changes in probe indicated temperature of $\leq 0.15K$ across the range of Mach numbers investigated. This value is comparable with the experimental uncertainty of $\sim 0.1K$ in the calculated temperature change. As a consequence, the low conductivity acrylic design significantly reduces the impact of unsteady effects on stagnation temperature probe performance. Accurate post-test corrections can therefore be applied to probe measurements based on steady aerodynamic calibration data.

By displaying insensitivity to unsteady effects, the acrylic PRT probe eliminates the dominant source of uncertainty that was associated with the standard PRT Kiel. In turbomachinery applications, this would result in further improvements in the accuracy of calculated component efficiencies. Assuming only the fundamental PRT sensing uncertainty of $0.15K$ ($0.05\%T0_\infty$) remains, Fig. 18 shows that the target accuracy of $\pm 0.5\%$ in component efficiency can now be achieved for all pressure ratios ≥ 1.5. This represents a major improvement compared to the other probes considered in this investigation. To achieve the highest stagnation temperature accuracy, probes with low susceptibility to conductive heat losses that also employ PRT sensors should therefore be employed for engine testing. Although the acrylic probe described here may not be sufficiently robust for such applications, alternative devices such as the dual-skin probe have already been demonstrated for this purpose [22].

7 CONCLUSION

This work has considered the performance of stagnation temperature probes in unsteady flows, typical of those produced by the wakes of rotating turbomachinery. It has been shown that probe performance undergoes changes between equivalent steady and unsteady flow conditions. This change is insensitive to the frequency of unsteadiness for values $> 1\,Hz$ due to the low dynamic response of the temperature sensor ($\tau \sim 1\,s$). However, it is characterised by a relative increase in the shortfall between the probe measured temperature and the average flow stagnation temperature in the unsteady case. As a result, temperature recovery ratios determined from steady aerodynamic calibrations cannot accurately be used to correct stagnation temperature measurements acquired from probes in unsteady wake flows. For conventional Kiel probes used in turbomachinery applications, this limits the achievable stagnation temperature uncertainty to $\geq 0.1\%T0_\infty$ and necessarily constrains the accuracy of subsequent component performance calculations. The changes in probe performance observed in unsteady flows have been attributed to increases in the conductive heat flux from the sensor to the surrounding probe body. This is caused by a non-linear relationship between the flow Mach number and the driving temperature gradient, which leads to a larger gradient in an unsteady flow compared to an equivalent steady flow (equal $\bar{M}_\infty$, $\bar{T0}_\infty$). The effect is expected to be greatest where there is a large Mach number deficit in the wake, and where the wake extends across a large percentage of the circumferential blade pitch. The increase in conductive heat flux is an order of magnitude larger than the variation in convective heat flux (or h), which has previously been identified in the literature as the leading physical mechanism responsible for unsteady effects. To reduce the impact of unsteadiness on stagnation temperature probe performance, it is therefore recommended that designs with low sensitivity to conduction be employed. This approach is preferable to attempting corrections for unsteady effects, which are complicated by their sensitivity to wake characteristics and subject to large uncertainties due to the inherent difficulties in quantifying unsteady flows. When adopting a low conduction design, it has proved possible to apply accurate post-test corrections based on aerodynamic calibration data, since the shortfalls between probe measured temperature and flow stagnation temperature remain unchanged between corresponding steady and unsteady flow conditions. A reduction in stagnation temperature uncertainty to $0.05\%T0_\infty$ can consequently be achieved, which allows turbomachinery component efficiency to be assessed to within $\pm 0.5\%$ over the full range of pressure ratios present in a high-bypass ratio turbofan engine. This represents a major improvement in comparison to conventional probe designs, which cannot achieve this accuracy for typical fan pressure ratios < 2.

8 ACKNOWLEDGEMENTS

This research was funded by the European Commission under the Framework 7 STARGATE project. The authors would like to thank Mark Erlund and Richard Stevenson from Rolls-Royce plc. for their contribution to the work.

References

[1] Bonham, C., Thorpe, S., Erlund, M., and Stevenson, R., 2017. "Combination probes for stagnation pressure and temperature measurements in gas turbine engines". *Measurement Science and Technology*.

[2] Saravanamuttoo, H., 1990. Recommended practices for measurement of gas path pressures and temperatures for performance assessment of aircraft turbine engines and components. Tech. rep., Defense Technical Information Centre.

[3] Moffat, R. J., 1962. "Gas temperature measurement". In Temperature: Its Measurement and Control in Science and Industry, Vol. 1, p. 553.

[4] Kupferschmied, P., Köppel, P., Gizzi, W., Roduner, C., and Gyarmathy, G., 2000. "Time-resolved flow measurements with fast-response aerodynamic probes in turbomachines". *Measurement Science and Technology,* ***11***(7), p. 1036.

[5] Sieverding, C., Arts, T., Dénos, R., and Brouckaert, J.-F., 2000. "Measurement techniques for unsteady flows in turbomachines". *Experiments in Fluids,* ***28***(4), pp. 285–321.

[6] Moffat, R. "Wake interaction effects and performance characteristics of stagnation-type thermocouples". In *Elemental design and development of small centrifugal compressor*, A. Welliver and J. Acurio, eds.

[7] Nabavi, M., 2010. "Invited review article: Unsteady and pulsating pressure and temperature: A review of experimental techniques". *Review of Scientific Instruments,* ***81***(3), p. 031101.

[8] Villafañe, L., and Paniagua, G., 2013. "Aerothermal analysis of shielded fine wire thermocouple probes". *International Journal of Thermal Sciences,* ***65***, pp. 214–223.

[9] Ng, W., and Epstein, A., 1983. "High-frequency temperature and pressure probe for unsteady compressible flows". *Review of Scientific Instruments,* ***54***(12), pp. 1678–1683.

[10] Buttsworth, D., and Jones, T., 1998. "A fast-response total temperature probe for unsteady compressible flows". *Journal of Engineering for Gas Turbines and Power,* ***120***(4), pp. 694–702.

[11] Kidd, S., Barton, J., Meredith, P., Jones, J., Cherrett, M., and Chana, K., 1995. "A fiber optic probe for gas total temperature measurement in turbomachinery". *Journal of turbomachinery,* ***117***(4), pp. 635–641.

[12] Allen, M. G., 1998. "Diode laser absorption sensors for gas-dynamic and combustion flows". *Measurement Science and Technology,* ***9***(4), p. 545.

[13] Agnew, B., Elder, R., and Terrel, M., 1985. "An investigation of the response of temperature sensing probes to an unsteady flow field". In ASME 1985 International Gas Turbine Conference and Exhibit, American Society of Mechanical Engineers, pp. V001T03A061–V001T03A061.

[14] Bianchini, A., Ferrara, G., Ferrari, L., Ballarini, V., Bianchi, L., Tapinassi, L., and Toni, L., 2012. "Effects due to the temperature measurement section on the performance estimation of a centrifugal compressor stage". *Journal of Engineering for Gas Turbines and Power,* ***134***(3), p. 032402.

[15] Timmerman, B., Skeen, A., Bryanston-Cross, P., and Graves, M., 2009. "Large-scale time-resolved digital particle image velocimetry (tr-dpiv) for measurement of high subsonic hot coaxial jet exhaust of a gas turbine engine". *Measurement Science and Technology,* ***20***(7), p. 074002.

[16] Coleman, H. W., and Steele, W. G., 1995. "Engineering applications of experimental uncertainty analysis". *The American Institute of Aeronautics and Astronautics Journal,* ***33***(10), pp. 1888–1896.

[17] Olczyk, A., 2008. "Problems of unsteady temperature measurements in a pulsating flow of gas". *Measurement Science and Technology,* ***19***(5), p. 055402.

[18] Bergman, T. L., Lavine, A. S., Incropera, F. P., and Dewitt, D. P., 2011. *Fundamentals of heat and mass transfer*. John Wiley & Sons New York.

[19] Cumpsty, N., and Horlock, J., 2006. "Averaging nonuniform flow for a purpose". *Journal of Turbomachinery,* ***128***(1), pp. 120–129.

[20] Bonham, C., Thorpe, S. J., Erlund, M. N., and Stevenson, R. D., 2013. "Stagnation temperature measurement using thin-film platinum resistance sensors". *Measurement Science and Technology,* ***25***(1), p. 015101.

[21] Zeisberger, A., 2007. "Total temperature probes for turbine and combustor applications". *Int. Society for Air Breathing Engines*.

[22] Thorpe, S. J., Bonham, C., and Erlund, M. N., 2016. Total temperature probe, Jan. 26. US Patent 9,243,963.

Table 1. TEST CONDITIONS.

M_i	M_o	$\frac{M_o}{M_i}$	$\frac{T_o}{T_i}$	$\frac{T0_o}{T0_i}$
0.25	0.3	1.20	0.99	1.0
0.35	0.3	0.86	1.01	1.0
0.45	0.3	0.67	1.02	1.0
0.55	0.3	0.55	1.04	1.0
0.65	0.3	0.46	1.07	1.0
0.75	0.3	0.40	1.09	1.0
0.85	0.3	0.35	1.12	1.0

Table 2. EXPERIMENTAL UNCERTAINTIES AT 95 % CONFIDENCE ($M_o/M_i = 0.5$, 50/50 DUTY CYCLE).

variable	systematic	random	expanded
T_b (K)	0.02	0.01	0.02
$T0_i$ (K)	0.07	0.01	0.08
$T0_o$ (K)	0.03	0.01	0.03
$P0_i$ (mbar)	0.3	2.0	2.0
$P0_o$ (mbar)	0.2	2.0	2.0
P_∞ (mbar)	0.2	2.0	2.0
R_T (%)	0.02	0.004	0.02
$\bar{M}_\infty$	0.005	0.004	0.006

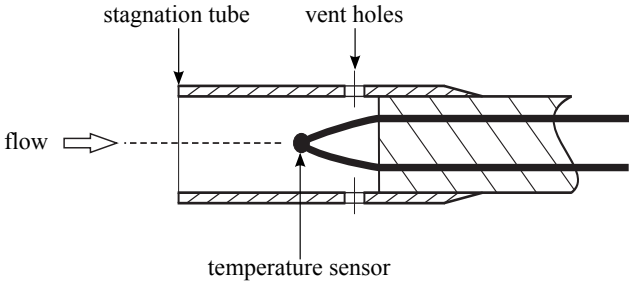

Fig. 1. DIAGRAM OF A THERMOCOUPLE KIEL PROBE.

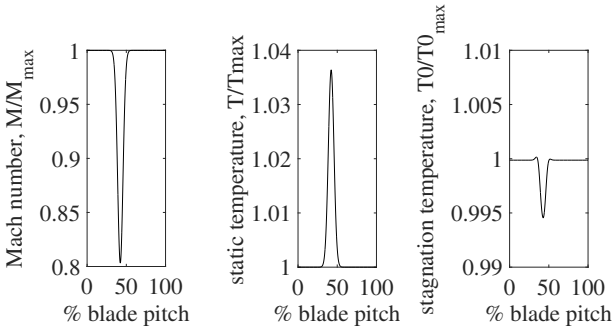

Fig. 2. NORMALISED FLOW PROFILES DOWNSTREAM OF THE FAN OF A HIGH-BYPASS RATIO TURBOFAN ENGINE.

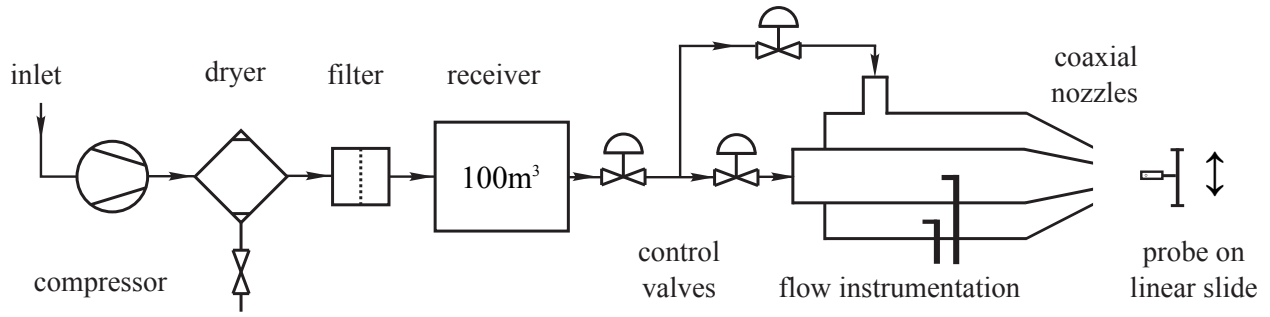

Fig. 3. TEST FACILITY.

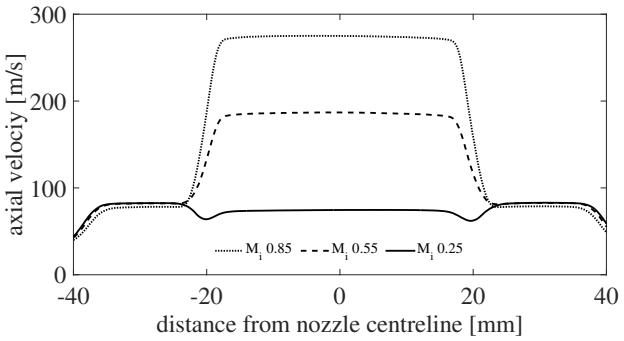

Fig. 4. AXIAL VELOCITY PROFILE AT COAXIAL NOZZLE EXIT FOR $M_i = 0.85,\ 0.55,\ 0.25$ AND $M_o = 0.3$

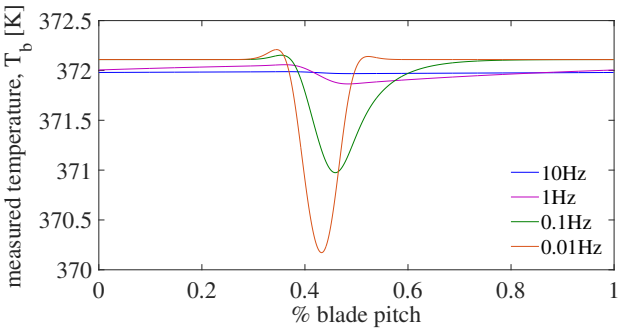

Fig. 5. FREQUENCY SENSITIVITY OF A $\varnothing$0.5 MM N-TYPE THERMOCOUPLE BEAD TO TYPICAL FLOW CONDITIONS DOWNSTREAM OF A FAN (f $0.01 - 10\,Hz$).

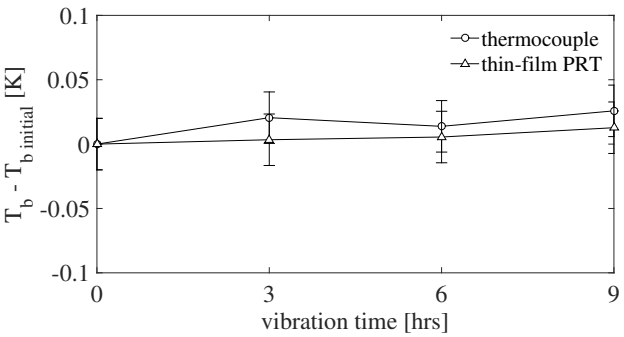

Fig. 6. IMPACT OF PROBE TRANSLATION ON SENSOR STATIC CALIBRATION RETENTION.

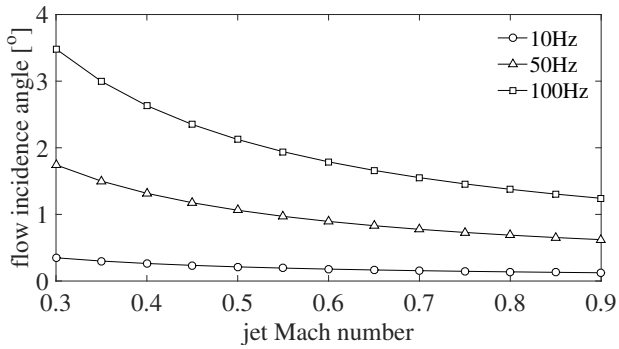

Fig. 7. INDUCED FLOW INCIDENCE ANGLE DUE TO PROBE TRANSLATION.

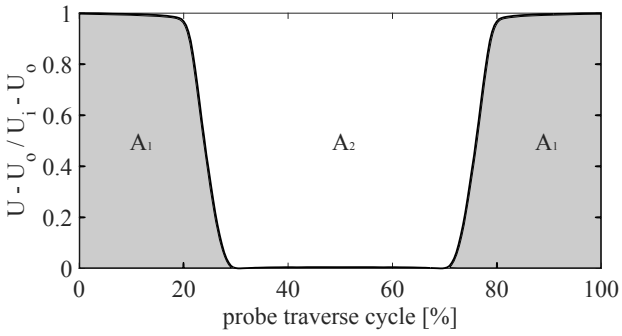

Fig. 8. NON-DIMENSIONALISED JET VELOCITY OVER ONE PROBE TRAVERSE CYCLE (50/50 DUTY CYCLE).

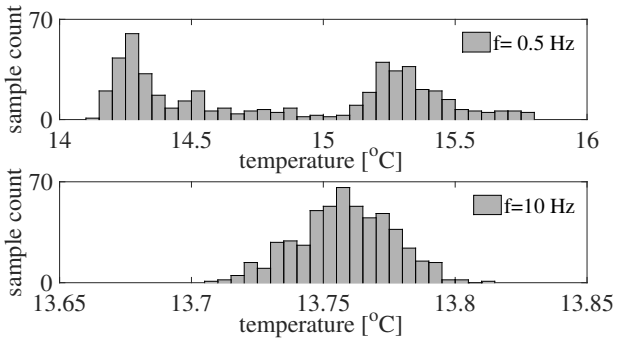

Fig. 9. HISTOGRAMS OF THERMOCOUPLE INDICATED TEMPERATURE AT $f = 0.5\,Hz$ AND $f = 10\,Hz$ ($M_o/M_i = 0.33$).

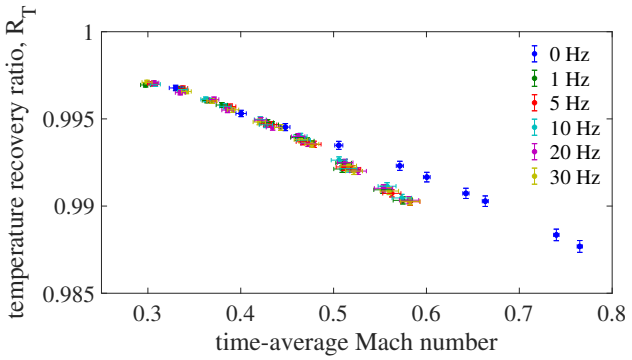

Fig. 10. TEMPERATURE RECOVERY RATIO OF THERMOCOUPLE KIEL PROBE FOR VARIOUS OSCILLATION FREQUENCIES (50/50 DUTY CYCLE).

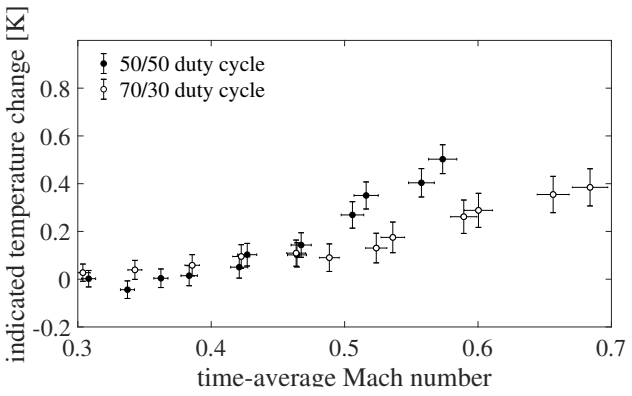

Fig. 11. CHANGE IN TEMPERATURE INDICATED BY THERMOCOUPLE KIEL PROBE BETWEEN $f = 0\,Hz$ AND $f = 10\,Hz$ FOR 50/50 AND 70/30 DUTY CYCLES.

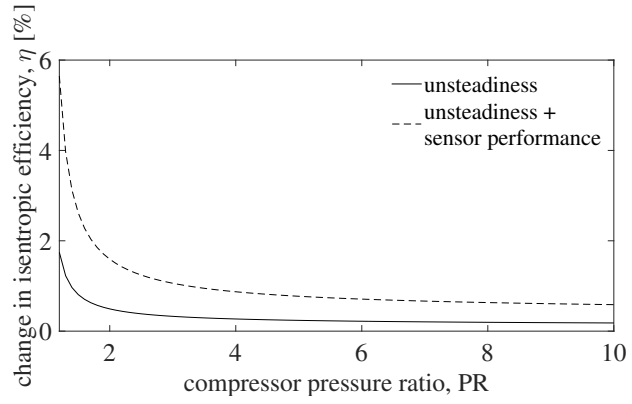

Fig. 12. IMPACT OF THERMOCOUPLE KIEL STAGNATION TEMPERATURE UNCERTAINTIES ON THE CALCULATED ISENTROPIC EFFICIENCY OF A COMPRESSOR ($T0_{in} = 300\,K$), $\eta_p = 0.85$.

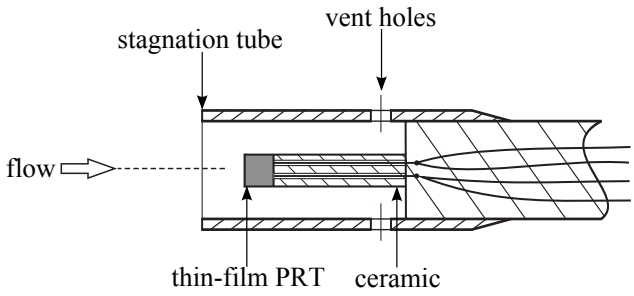

Fig. 13. DIAGRAM OF A PRT KIEL PROBE.

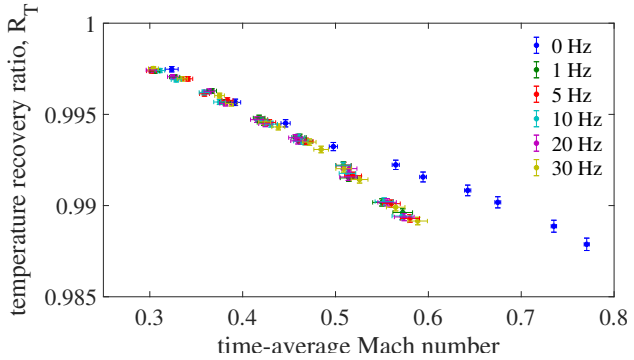

Fig. 14. TEMPERATURE RECOVERY RATIO OF PRT KIEL PROBE FOR VARIOUS OSCILLATION FREQUENCIES (50/50 DUTY CYCLE).

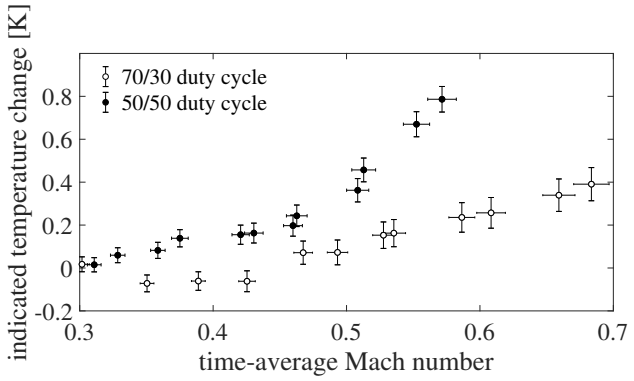

Fig. 15. CHANGE IN TEMPERATURE INDICATED BY PRT KIEL PROBE BETWEEN $f = 0\,Hz$ AND $f = 10\,Hz$ FOR 50/50 AND 70/30 DUTY CYCLES.

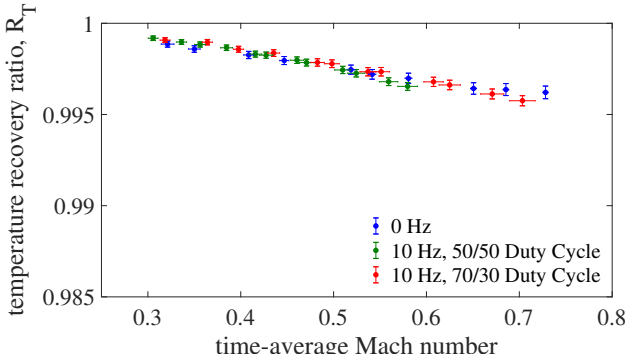

Fig. 16. TEMPERATURE RECOVERY RATIO OF ACRYLIC KIEL PROBE AT $f = 10Hz$ (50/50 AND 70/30 DUTY CYCLES).

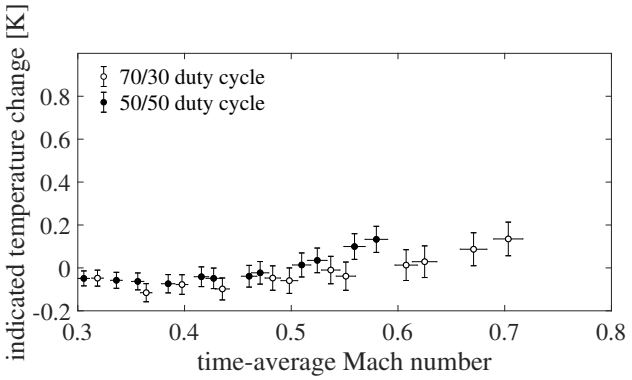

Fig. 17. CHANGE IN TEMPERATURE INDICATED BY ACRYLIC KIEL PROBE BETWEEN $f = 0Hz$ AND $f = 10Hz$ FOR 50/50 AND 70/30 DUTY CYCLES.

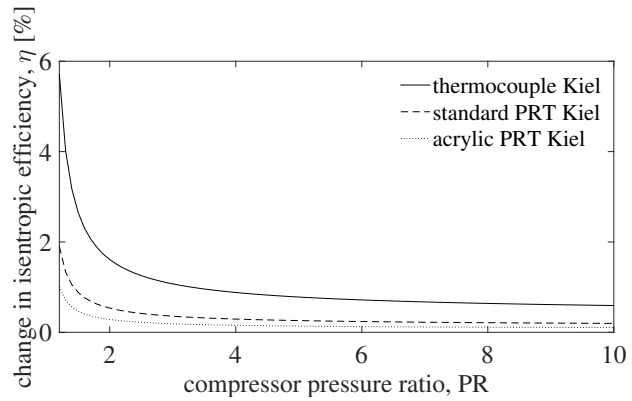

Fig. 18. IMPACT OF COMBINED STAGNATION TEMPERATURE UNCERTAINTIES FOR ALL THREE PROBES ON THE CALCULATED ISENTROPIC EFFICIENCY OF A COMPRESSOR ($T0_{in} = 300K$), $\eta_p = 0.85$.